

ARTICLE

## Experimental Investigation on the Mechanical Properties of Silicone Elastomers Filled with Fumed Silica for Seismic Isolation Bearings

Arthur Ramandalina \* , Ji Dang 

Graduate School of Science and Engineering, Saitama University, Saitama 338-8570, Japan

### ABSTRACT

Laminated elastomeric bearings used in seismic isolation rely on the mechanical properties of their constituent elastomers to ensure effective performance. However, despite their resistance to temperature fluctuations and environmental aggressors, silicone elastomers exhibit relatively low stiffness, limiting their direct applicability in seismic isolation. This study investigates the effect of fumed silica as a reinforcing filler to enhance the mechanical properties of laminated silicone elastomeric bearings. Elastomeric samples were fabricated with varying fumed silica proportions and subjected to Shore A hardness, uniaxial tensile, and lap shear tests to assess the influence of filler content. Additionally, quasi-static tests were conducted on reduced-scale bearing prototypes under combined vertical compression and cyclic horizontal shear to evaluate their seismic isolation performance. The results demonstrate that fumed silica reinforcement significantly increases stiffness, as evidenced by higher Shore A hardness values. However, a trade-off was observed in tensile properties, with reductions in tensile strength and elongation at break. Despite this, the equivalent elastic modulus did not show substantial variation up to large deformations, indicating that stiffness is preserved under most working conditions. Lap shear tests showed that fumed silica improves shear resistance, while quasi-static tests revealed inelastic behavior with small increases in equivalent shear coefficients but no substantial loss in damping ratios. These findings suggest that fumed silica reinforcement enhances silicone elastomers' stiffness and shear resistance while maintaining moderate damping properties, making it a promising approach for improving the mechanical performance of elastomeric bearings in seismic isolation applications.

**Keywords:** Silicone Elastomer; Fumed Silica; Elastomeric Bearing; Seismic Isolation; Experimental Study

#### \*CORRESPONDING AUTHOR:

Arthur Ramandalina, Graduate School of Science and Engineering, Saitama University, Saitama 338-8570, Japan; Email: miharivoarthur@gmail.com

#### ARTICLE INFO

Received: 18 January 2024 | Revised: 19 February 2025 | Accepted: 24 January 2025 | Published Online: 6 March 2025

DOI: <https://doi.org/10.30564/jbms.v7i1.8472>

#### CITATION

Ramandalina, A., Dang, J., 2024. Experimental Investigation on the Mechanical Properties of Silicone Elastomers Filled with Fumed Silica for Seismic Isolation Bearings. *Journal of Biomedical Science*. 7(1): 44–61. DOI: <https://doi.org/10.30564/jbms.v7i1.8472>

#### COPYRIGHT

Copyright © 2025 by the author(s). Published by Bilingual Publishing Group. This is an open access article under the Creative Commons Attribution-NonCommercial 4.0 International (CC BY-NC 4.0) License (<https://creativecommons.org/licenses/by-nc/4.0/>).

## 1. Introduction

The safety and resilience of urban infrastructure in earthquake-prone regions rely heavily on seismic isolation systems designed to protect structures from damage during seismic events<sup>[1–3]</sup>. Among the existing vibration control technologies, seismic base isolation, which belongs to the passive vibration control category, has gained popularity due to its relatively low cost<sup>[4, 5]</sup>. In this collection, plain and laminated elastomeric bearings have been extensively used to mitigate seismic forces by absorbing and dissipating energy, thereby reducing the vibrations transmitted to the superstructure<sup>[2, 6]</sup>. These bearings, typically constructed from rubbers reinforced with fillers, are widely used owing to their enhanced mechanical properties like stiffness, tensile strength, and energy dissipation capacity<sup>[1, 6]</sup>.

Conventional elastomeric materials such as natural and high-damping rubber have been extensively employed in seismic isolation systems. However, achieving optimal performance under extreme conditions remains a significant challenge. For instance, conventional elastomers may exhibit reduced efficiency when subjected to extreme ambient temperatures or prolonged exposure to certain environmental factors, which can compromise their long-term durability and reliability in harsh environments<sup>[7–10]</sup>. These limitations necessitate exploring alternative materials to overcome these shortcomings while maintaining or improving seismic isolation performance.

In this context, silicone elastomers have gained increasing attention as promising alternatives to seismic isolation elastomers. Their natural resistance to temperature fluctuations and chemical inertness, which allows them to resist oxidative degradation, ozone exposure and other environmental aggressions, makes them particularly suitable for long-term use in environments characterized by severe weather conditions or significant temperature variations<sup>[11–13]</sup>. Unlike conventional rubbers requiring complex vulcanization, silicone elastomers can be cured at room temperature without high temperature or pressure. This flexibility can drastically simplify the fabrication process and reduce substantial manufacturing costs<sup>[14]</sup>. However, despite these advantages, unmodified silicone elastomers' relatively low tensile strength and stiffness present critical limitations for their direct application in seismic isolation systems<sup>[15, 16]</sup>. This drawback highlights the need for innovative strategies to enhance their

mechanical properties while preserving their inherent benefits.

A widely used approach to improving the mechanical properties of elastomers involves incorporating reinforcing fillers. Among the various fillers used to reinforce elastomeric materials, fumed silica has emerged as an effective agent for improving the performance of silicone elastomers<sup>[17, 18]</sup>. The large surface area and high surface energy of fumed silica enable it to interact with the polymer matrix at the molecular level, forming a robust network structure that enhances the overall mechanical properties of the material<sup>[19–21]</sup>. The incorporation of fumed silica has been shown to improve properties like the equivalent elastic modulus, tear strength, and fatigue resistance, making it a promising reinforcement for developing high-performance elastomeric materials<sup>[22–24]</sup>.

Several studies have investigated the effects of incorporating fumed silica into elastomers, consistently reporting improvements in stiffness, tensile modulus, and fatigue resistance<sup>[21, 25–27]</sup>. However, while much research has focused on improving the general mechanical properties of these materials, there remains a lack of studies investigating the effects of fumed silica reinforcement on the seismic isolation performance of laminated silicone elastomeric bearings, particularly in terms of energy dissipation capacity, shear modulus, and damping capacity.

This study addresses the following research question: how does incorporating fumed silica as a reinforcing filler influence the mechanical and seismic isolation performance of laminated silicone elastomeric bearings? The following hypotheses are proposed based on previous studies and the mechanical behavior of reinforced elastomers. (1) Increasing fumed silica content will enhance the stiffness of silicone elastomers, as evidenced by higher Shore A hardness values. (2) Incorporating fumed silica will reduce the tensile strength and elongation at break due to increased material stiffness. (3) Reinforced silicone elastomers will exhibit improved shear performance, with increased equivalent shear modulus and damping capacity under quasi-static loading conditions.

Hence, this study aims to investigate the effect of fumed silica as a reinforcing filler in laminated silicone elastomeric bearings for seismic isolation applications. Specifically, the research focuses on evaluating the influence of varying filler

proportions on stiffness, tensile behavior, and shear performance through mechanical testing and analyzing the quasi-static response of reduced scale bearing prototypes under combined vertical compression and cyclic horizontal shear.

This research provides theoretical insights into the role of fumed silica as a reinforcing filler in silicone elastomers, contributing to the understanding of material modification strategies for seismic isolation applications. By assessing the mechanical behavior of fumed silica-reinforced elastomers under relevant loading conditions, the study helps clarify the trade-offs between stiffness, ductility, and energy dissipation, offering a scientific basis for optimizing elastomer formulations.

From a practical perspective, the findings contribute to the development of high-performance elastomeric bearings capable of maintaining mechanical integrity and seismic isolation performance under extreme environmental and weather conditions. Understanding the impact of filler content on shear modulus and damping properties allows refinements of material formulations for the next generation of elastomeric bearings, ensuring greater durability and resilience of structures in earthquake-prone regions.

The methodology section of this paper details the material selection, sample fabrication, and testing procedures. The results obtained from mechanical and quasi-static tests are presented in the subsequent section, followed by an interpretation of their implications for seismic isolation. The paper concludes with a summary of key findings and directions for future research.

## 2. Literature Review

### 2.1. Reinforcing Filler for Silicone Elastomers

Research on the mechanical enhancement of elastomeric materials through filler reinforcement has been widely explored in material science and engineering. Several studies have investigated the role of reinforcing fillers such as carbon black, silica, and nanoparticles in improving the mechanical properties of elastomers used in various applications<sup>[28–30]</sup>. Among these, fumed silica has emerged as a promising reinforcing agent for silicone elastomers due to its ability to increase stiffness and modulus while maintaining flexibility<sup>[31, 32]</sup>.

Originally introduced as a means of reducing produc-

tion costs, fillers play a pivotal role in increasing the hardness and enhancing tensile strength, tear resistance, damping performance, and abrasion resistance of elastomer matrices<sup>[28–30]</sup>. They can improve mechanical properties by reinforcing the elastomer, leading to increased strength, abrasion resistance, and tear resistance, with fillers like carbon black being very effective<sup>[33]</sup>. Fillers also reduce material costs by replacing part of the polymer with cheaper substances like calcium carbonate or clay. Additionally, they can ease the processability of elastomers, making them easier to handle and shape during manufacturing<sup>[12, 25]</sup>.

A preliminary study was conducted to assess the available fillers, their potential effects, and their incorporation levels. The key fillers considered included silica, carbon black, and other nano-sized particulates, each offering unique advantages<sup>[12, 25, 33]</sup>. Carbon black has been widely used for enhancing tensile strength and tear resistance in rubber composites<sup>[34, 35]</sup>, while other nano-fillers, such as clay-based reinforcements, have been explored for improving damping properties<sup>[36, 37]</sup>. However, fumed silica stands out among the available fillers due to its high surface area, amorphous structure, and intense interaction with silicone matrices. Its inorganic structure, reproducible dispersion properties, and compatibility with silicone elastomers make it an ideal candidate for enhancing material stiffness while preserving chemical inertness and processability. Several studies have focused on the effects of fumed silica on the mechanical behavior of silicone elastomers. Incorporating fumed silica into silicone elastomers significantly enhances stiffness, tensile modulus, and tear strength by improving the formation of a strong interfacial interaction between the polymer matrix and filler particles<sup>[38]</sup>. Similarly, Jiang and Yong<sup>[31]</sup> reported that an optimized distribution of fumed silica in silicone elastomers leads to an increase in equivalent elastic modulus without severely compromising elongation at break.

In seismic isolation, filler reinforcement strategies have been explored to improve the performance of elastomeric bearings. Abedi Koupai, Bakhshi and Valadoust Tabrizi<sup>[39]</sup> investigated the impact of carbon black on the shear behavior of styrene butadiene rubber bearings, demonstrating an improvement in shear modulus and damping properties. However, incorporating carbon black can sometimes increase the material's brittleness, mainly in lower temperatures, where it may reduce ductility. In addition, high levels of carbon black

can impede workability by thickening the elastomer, which can require adjustments in the processing conditions<sup>[40, 41]</sup>. Its opaque nature also eliminates transparency, complicating visual inspection of internal layers, which represents a drawback in contexts where nondestructive inspection methods are essential<sup>[42–44]</sup>.

Regarding shear performance, prior research has emphasized the need to balance stiffness enhancement with damping properties. Haddad et al.<sup>[45]</sup> explored the effect of nanoparticle-reinforced rubber composites in vibration isolation applications and reported that while increasing filler content leads to improved stiffness, it may also reduce damping efficiency, which is critical for energy dissipation. This finding aligns with observations by Jin et al.<sup>[46]</sup>, who noted that excessive reinforcement may increase brittleness and reduce shear compliance, posing challenges in seismic isolation applications.

Although these studies provide valuable insights into filler reinforcement strategies and filled rubber material behavior, limited research has been conducted on the specific effect of fumed silica on the seismic isolation performance of silicone elastomeric bearings. The influence of varying filler proportions on key parameters such as equivalent shear modulus, damping ratio, and energy absorption capacity remains an open question, which will be addressed in this study.

## **2.2. Novelty and Contributions to Science**

This study presents an investigation into the effects of fumed silica reinforcement on the mechanical and seismic isolation performance of laminated silicone elastomeric bearings. While the use of silicone elastomers in seismic isolation has been previously suggested due to their superior environmental resistance, their relatively low stiffness and tensile strength have posed significant challenges for practical application. Although fumed silica has been widely recognized as a reinforcing filler for silicone-based materials, prior studies have primarily focused on its role in improving general mechanical properties such as tensile strength, tear resistance, and fatigue life. However, the specific influence of fumed silica reinforcement on the seismic isolation behavior of silicone elastomeric bearings, including shear moduli, damping characteristics, and energy dissipation capacity, remains largely unexplored.

Unlike conventional studies that focus on bulk silicone

elastomers, this research investigates the performance of laminated silicone elastomeric bearings, considering their structural application in seismic isolation. The study systematically examines the impact of varying fumed silica filler proportions (0, 1.25, and 2.50 phr) on Shore A hardness, uniaxial tensile strength, and shear properties, providing insights into the trade-offs between stiffness enhancement and material ductility. A novel aspect of this work is the inclusion of quasi-static tests on reduced-scale bearing prototypes, assessing their behavior under combined constant vertical compression and cyclic horizontal shear loading, which provides direct experimental validation of the material's effectiveness in seismic isolation applications.

The research goes beyond standard mechanical tests to evaluate key seismic parameters, such as equivalent shear coefficients and damping ratios, which are critical for practical implementation in base isolation systems. The study compares experimental results with established standard threshold values for elastomeric bearings, offering a useful perspective on the feasibility of using fumed silica-reinforced silicone elastomers in seismic isolation systems. By integrating material characterization with structural performance analysis, this research provides valuable insights for both material scientists developing high-performance elastomers and engineers designing next-generation seismic isolation systems.

## **3. Materials and Methods**

### **3.1. Research Methodology**

The research methodology follows a systematic approach to evaluate the effect of fumed silica reinforcement on the mechanical and seismic isolation performance of laminated silicone elastomeric bearings. The study consists of four main stages: (1) material selection and preparation, (2) sample fabrication, (3) experimental testing, and (4) data analysis and comparison.

A preliminary assessment of potential fillers was conducted, leading to the selection of fumed silica due to its high surface area, amorphous structure, and higher interaction with silicone matrices. The filler content was limited to 2.50 phr to guarantee a homogenous dispersion within the matrix. Elastomeric samples were fabricated with different filler proportions (0 phr, 1.25 phr, and 2.50 phr), ensuring con-

trolled processing conditions to maintain consistency across test specimens. These samples were subjected to mechanical testing, including Shore A hardness, uniaxial tensile, and lap shear tests, to assess their stiffness, tensile properties, and shear behavior. Additionally, prototype bearings were tested under quasi-static shear loading conditions to evaluate their seismic isolation performance under combined vertical compression and cyclic horizontal shear. The collected data were analyzed to interpret the influence of filler content on key

parameters, including equivalent elastic modulus, shear modulus, and damping capacity. **Figure 1** presents a flowchart summarizing the methodology and the steps followed in this study and highlights the logical progression from material selection to final analysis, ensuring a structured approach to evaluating the effectiveness of fumed silica reinforcement in silicone elastomeric bearings. The subsequent subsections provide detailed descriptions of each stage of the methodology.

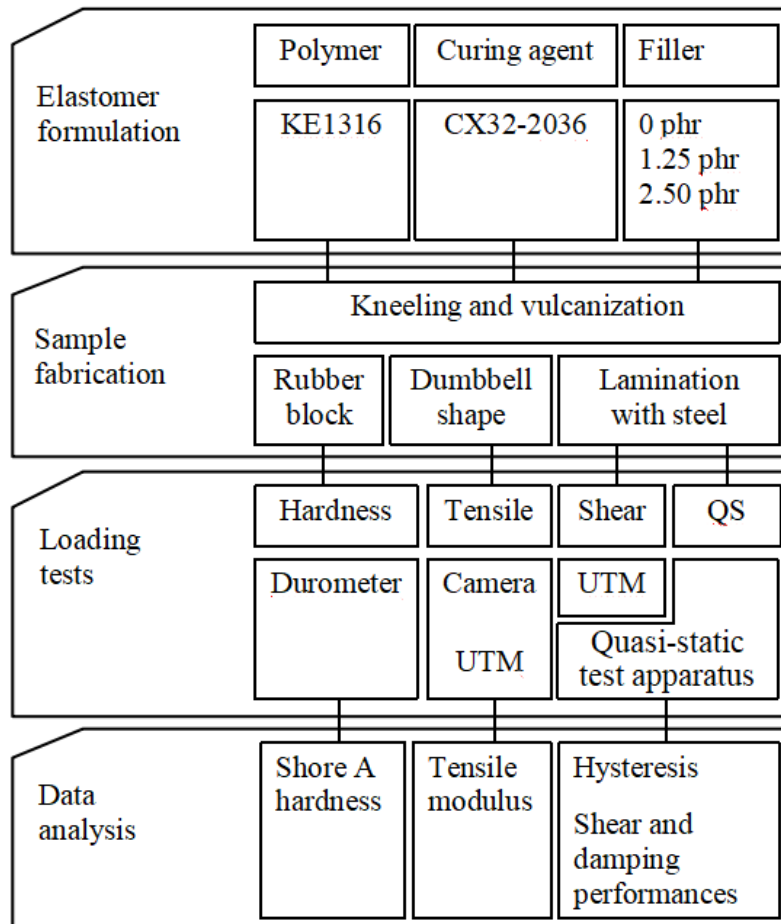


Figure 1. General flowchart of the research.

### 3.2. Elastomer Vulcanization and Sample Fabrication

The materials used in this study were selected to warrant a reliable and reproducible evaluation of the effects of fumed silica as a reinforcing filler in silicone elastomeric bearings. The base elastomers consisted of commercially available room-temperature vulcanizing silicone compounds chosen for their flexibility, workability, and accessibility.

The polymer matrices were obtained by curing the liquid KE1316 base polymer with the CX32-2036 curing agent, which was expected to result in relatively ductile elastomers. These matrices provided a consistent base for preparing samples with varying filler proportions.

The fumed silica powder is characterized by its highly porous, nanoscale particles with specific gravities ranging between 2.2 and 4.5 g mm<sup>-3</sup>. The individual particles typically have a grain size ranging from 9 to 55 nm, and the powder

possesses a high surface area averaging  $100 \text{ m}^2 \text{ g}^{-1}$  [47]. This large surface area provides a unique ability to form a network of particles that bond with the silicone polymer chains, thus mainly increasing the mechanical strength and modulus of the elastomer matrix, while the high porosity of the grains contributes to a better mechanical interlocking effect.

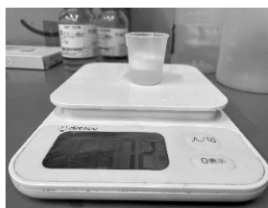
Three different proportions of fumed silica were incorporated to investigate the influence of filler loading: 0 phr for the control samples, 1.25 phr, and 2.50 phr. These filler proportions were selected to encompass a range of low to moderate reinforcement levels while maintaining optimal workability.

The fabrication of elastomer samples for experimental testing, summarized in **Figure 2**, was carried out in ordered processes to ensure consistent, reproducible, and reliable results across all formulations. The weight of each raw compound was measured by a precision weighing machine according to the desired formulations: the polymer and curing agent were combined at a predetermined ratio, following the manufacturer recommendations for optimal curing, and fumed silica was added in varying amounts to test the effect of filler concentration on the properties of the resulting elastomer.

Once the weights of the raw compounds were measured, they were thoroughly mixed at a mixing rate of 200 rpm to ensure homogeneity and to disperse the filler material

evenly throughout the raw mixture.

After mixing, the liquid polymer compound was poured into appropriate recipients to prepare sheets for use in uniaxial tensile and to make blocks for Shore A hardness tests. The fluid mixture was spread evenly to a consistent thickness, ensuring uniformity in the sample preparation. The mixed blend was then placed into a vacuum chamber to remove entrapped air bubbles, which could affect the consistency of the final elastomer. The mixing speed and deaeration duration were optimized to achieve a smooth, even, and uniform mixture that would cure properly without unwanted air pockets. Instead of leaving them in an open-air environment for precision and reproducibility, the prepared molds were placed in a low-temperature incubator at a fixed temperature of  $23 \text{ }^\circ\text{C}$  to initiate the curing process. Curing time and temperature were controlled to ensure proper crosslinking of the silicone elastomer while ensuring uniformity and reproducibility of the experimental data. After the initial curing, the vulcanized elastomers can be subjected to a post-curing process, which was omitted in this study. This optional process involved placing the samples in the oven at a slightly elevated temperature for an extended period, typically 2 to 4 hours at  $50 \text{ }^\circ\text{C}$ , to ensure that the elastomers reached their full mechanical potential and to remove any volatile and residual solvents or unreacted polymers that could affect performances.



**1- MIXING**

Mix the raw materials in proportion and knead until homogenous.



**2- DEFOAMING**

Remove entrapped air bubbles.



**3- VULCANIZATION**

Let the raw elastomer cure for 24 hours in a low-temperature incubator.



**4- CONDITIONING**  
*(Optional)*

Subject the resulting elastomer to controlled heat.

**Figure 2.** Elastomer fabrication process.

The numbering of the test batches was done straightforwardly and logically. The first characteristic identified the test type: H for hardness, T for tensile, L for lap shear, and P for quasi-static shear tests. The second characteristic represents the filler proportion, as summarized in **Table 1**. For the lamination process, SS400 steel rods and plates were prepared according to specified designs and dimensions to serve as reinforcing components, providing the necessary structural support to the elastomeric parts. Twelve samples were prepared for each test batch to ensure reproducibility and avoid singular test results, with the exception of the bearing prototypes, where one prototype per batch was fabricated.

**Table 1.** Nomenclature of test batches.

No.	Silicone Material	Curing Agent	Filler (phr)
1	KE1316	CX32-2036	0
2	KE1316	CX32-2036	1.25
3	KE1316	CX32-2036	2.50

### 3.3. Shore A Hardness, Tensile, and Lap Shear Tests

#### 3.3.1. Shore A Hardness Tests

Shore A hardness tests were conducted to evaluate the stiffness of the elastomer samples according to ASTM D2240 standards<sup>[48]</sup>. The testing procedure involved applying a calibrated durometer, shown in **Figure 3**, to elastomer blocks with dimensions adhering to standard specifications. The durometer, equipped with a Type A indenter, designed for measuring the hardness of soft elastomers and rubber-like materials, was selected due to its accuracy in determining the indentation resistance of materials that have relatively low stiffness, including silicone elastomers.



**Figure 3.** Hardness Shore A durometer.

The samples were categorized into three batches of elastomers fabricated using the KE1316 base polymer cured with CX32-2036 and filled with fumed silica in proportions of 0 phr, 1.25 phr, and 2.50 phr.

The durometer was applied perpendicularly to the sample surface during the test, and the hardness was recorded. The hardness value was collected in a way that did not account for any occurring time-dependent recovery or elastic rebound of the elastomer due to its viscoelastic nature. Measurements were taken at five different locations across the surface of each sample, with a minimum distance of 6 mm between measurements to ensure the representativeness of the hardness values. This approach helped to account for any material heterogeneity or local variations in the properties of the elastomer. The arithmetic mean of the five measurements was calculated and recorded as the final Shore A hardness value for each elastomer formulation. The mean value provides a more accurate reflection of the overall hardness of the material while accounting for minor variations in the sample.

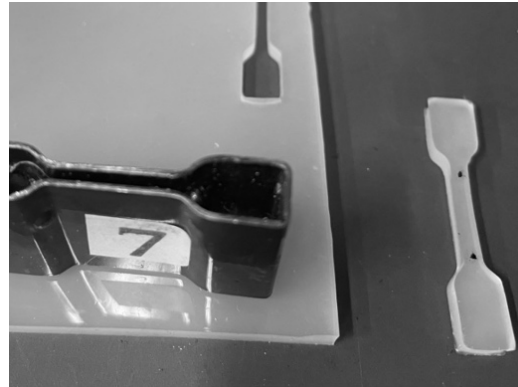
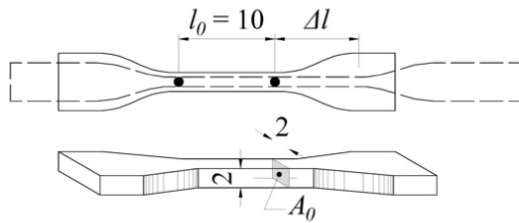
#### 3.3.2. Uniaxial Tensile Tests

Uniaxial tensile tests were performed to investigate the tensile behavior of the elastomer samples according to ASTM D412 standards<sup>[49]</sup> through the assessment of tensile strength, strain at break, and equivalent elastic modulus as key parameters. The samples were cut into dumbbell shapes using a cutting die corresponding to dumbbell shape No. 7 in JIS K 6251<sup>[50]</sup>. These samples were extracted from elastomer sheets prepared under the same conditions as those for the Shore A hardness test samples. Three batches (T1 through T3) were created, covering all combinations of the three filler proportions. The sample design and representative dumbbell-shaped samples are shown in **Figure 4**.

The tests were conducted using a tabletop tensile compression testing machine at a  $200 \text{ mm min}^{-1}$  test speed until rupture occurred, following the recommendation of the JIS K 651. A digital camera, which offers 4K video at 30 fps, providing excellent image stabilization and high optical zoom, was used to capture the deformation behavior of the samples during testing. The applied force was continuously recorded by the testing machine integrated measurement system. Simultaneously, the elongation was tracked using the video analysis system by measuring the movement of the two dots placed at the ends of the initial gauge length of the sample.

The deformation was recorded from pixel measurement of displacements, which was later converted into actual elongation values. The force data and elongation measurements

were combined to construct the nominal stress-strain curve, from which tensile strength and elongation strain at break were derived.



(a)

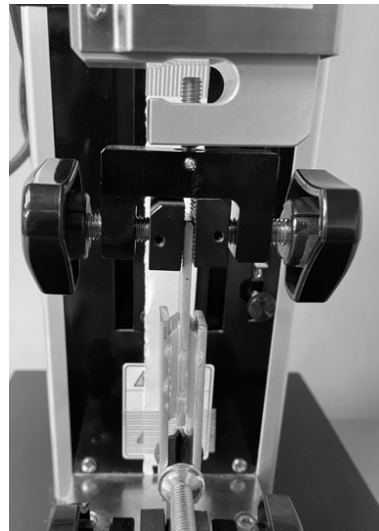
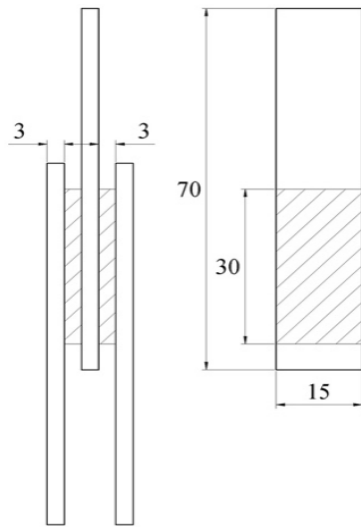
(b)

Figure 4. Dumbbell shape No.7: (a) dumbbell shape No.7 design (mm) and (b) test sample with its cutting die.

### 3.3.3. Lap Shear Tests

Double lap shear tests were conducted to evaluate the shear behavior of the laminated elastomer and were performed on double lap shear samples designed into Y-shaped specimens. Key parameters were shear strength, ultimate shear strain (corresponding to the shear strength), and equivalent shear modulus. Each test sample consisted of a lamination comprising two elastomer sheets bonded to three

SS400 steel plates. Both force and displacement data were collected from the universal testing machine integrated measurement system during testing. The tests were displacement-controlled with a  $10 \text{ mm min}^{-1}$  loading rate until failure occurred. This approach provided a steady rate of strain, ensuring that the failure mode was predominantly influenced by the mechanical properties of the assembly rather than its dynamic responses. The design of the test samples and a photograph of a tested specimen are shown in Figure 5.



(a)

(b)

Figure 5. Lap shear test sample: (a) sample design (mm) and (b) sample mounted on the testing machine.

### 3.4. Seismic Performance of Bearing Prototypes

Quasi-static tests were conducted on reduced-scale bearing prototypes to evaluate their mechanical performance under combined constant vertical compression and horizontal cyclic displacement. On top of the hysteresis loops, the equivalent shear coefficient and damping ratio were analyzed. The reduced size of the prototypes should not have any interference with the targeted mechanical properties because of their normalized characteristic. The tests were performed in the experimental building of the structural engineering laboratory at Saitama University, using a custom-designed loading apparatus illustrated in **Figure 6**. The loading setup consisted of two rigid reinforced metallic columns supporting a rigid metallic beam, on which a vertical actuator was mounted to apply the designed compressive load. A horizontal actuator was mounted on one of the columns to provide cyclic displacement during a displacement-controlled testing procedure. The bearing samples were mounted on a sliding rail system, positioned on top of a basement, and aligned with the vertical actuator to ensure frictionless testing.

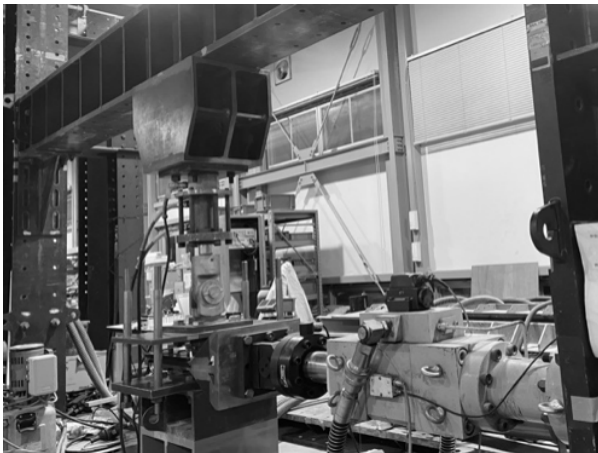


**Figure 6.** Quasi-static test loading apparatus.

During testing, the vertical actuator applied a constant compressive pressure of 6.00 MPa. Meanwhile, the horizontal actuator applied a cyclic displacement, following the displacement protocol illustrated in **Figure 7**, at a rate of 2 mm s<sup>-1</sup> until either rupture occurred or the third cycle at 250% strain was achieved. In addition, two laser displacement

sensors were mounted to monitor the displacement of the bearing loading plates. Key parameters recorded during the tests included the horizontal force-displacement relationship, vertical stiffness, and deformation behavior of the bearing under cyclic loading.

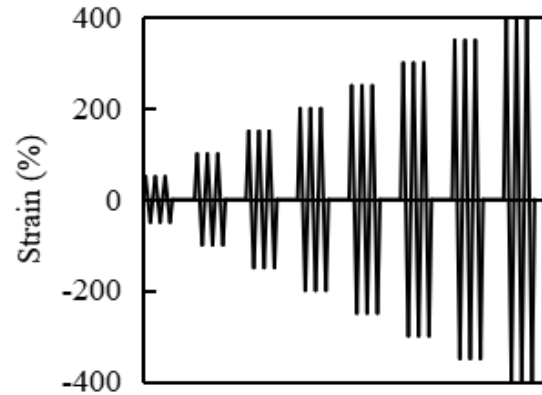


**Figure 7.** Quasi-static test loading amplitudes.

As depicted in **Figure 8**, the bearing prototypes used for these tests were square-shaped, with dimensions of 100 mm by 100 mm, providing a shear surface area of 10,000 mm<sup>2</sup>. The overall thickness of a bearing prototype was 45 mm, and it consisted of a structured layer assembly of four 3 mm thick silicone elastomer sheets alternated with three 1 mm thick steel plates. This laminated configuration was designed to optimize performance under compression and shear loading conditions.

Since shape factors can affect the ability of the prototype to resist compression and shear solicitations, their values, summarized in **Table 2**, were selected to provide optimal vertical and horizontal deformation resistances.

To complete the assembly, two outer steel loading plates, each 15 mm thick, were added to cover the laminated structure and ensure a firm bolted fixation to the loading apparatus. The prototypes were fabricated to withstand a design compression stress of 6.00 MPa and an ultimate compression stress of 9.00 MPa.

**Table 2.** Bearing prototype shape factors.

First Shape Factor	8.33
Second shape factor	8.33

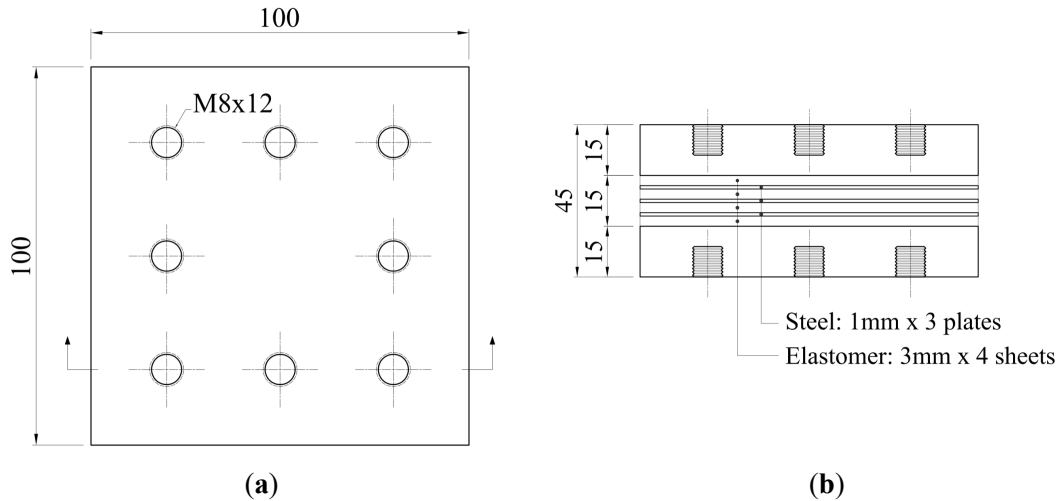


Figure 8. Quasi-static test prototype design (mm).

## 4. Results and Discussion

### 4.1. Shore A Hardness and Uniaxial Tensile Tests

#### 4.1.1. Shore A Hardness Tests

The Shore A hardness results provided insights into the stiffness of the tested silicone elastomers when influenced by fumed silica reinforcement. The results, visualized in **Figure 9**, demonstrate a clear correlation between the filler content and material stiffness. The hardness values increased consistently with filler proportion: the unfilled samples (H1) exhibited an average Shore A hardness of approximately 21, while samples with 1.25 phr and 2.50 phr showed hardnesses averaging 49 and 56, respectively.

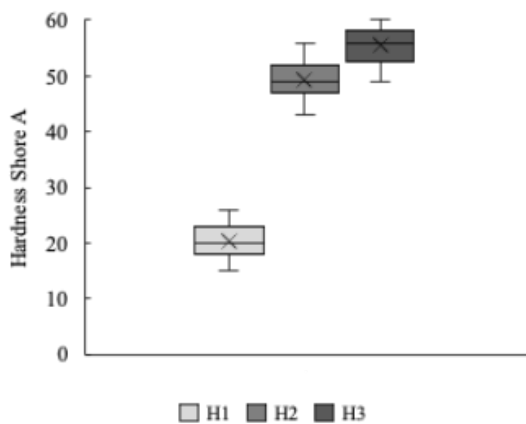


Figure 9. Shore A hardness test results.

Shore A hardness tests confirmed that incorporating

fumed silica increased the stiffness of the silicone elastomers. The apparent correlation between the hardness values and filler proportions demonstrates the reinforcing effect of fumed silica, attributed to its ability to form a robust network structure within the polymer matrix. The filler grains create chemical liaisons, which provide stronger chemical bonds between the crosslinked polymer chains. This phenomenon leads to an improvement in the material stiffness, which is favorable for bearing applications, where an enhanced stiffness can contribute to better load-bearing capacities and overall performance in seismic isolation systems.

#### 4.1.2. Uniaxial Tensile Tests

A summary of the averaged uniaxial tensile stress-strain relationships is shown in **Figure 10**. The unfilled samples (T1) recorded a tensile strength averaging 11.25 MPa, and incremental filler addition resulted in tensile strengths of 9.55 MPa and 8.50 MPa for T2 and T3, respectively. The elongation at break displayed an analogous trend, decreasing with increasing filler proportions. The unfilled samples reached a maximum strain of over 1,000%, while filled samples with 1.25 phr and 2.50 phr exhibited maximum strains of 900% and 800%, respectively. Yet, these strains are far above the minimum elongation at break of 450% recommended by the ASTM D412<sup>[49]</sup>.

Hence, these experiment results demonstrate that fumed silica reinforcement slightly reduces the tensile performance of the elastomer matrices. However, the equivalent elasticity moduli did not show substantial changes up to a

comprehensively large strain value. For instance, they averaged a value of 0.80 MPa for the unfilled elastomers and 0.90 MPa for elastomers with higher filler concentrations at 400% strain. These findings contrast with previous studies done by Jin et al.<sup>[46]</sup>, stipulating that, by means of a specific incorporation technique, the incorporation of silicon dioxide-based nanofillers at 2.50 phr in natural rubber can increase the tensile strength, elongation at break and equivalent elastic modulus by 11%, 18%, and 9%, respectively. However, they align with the work done by Jiang and Yong<sup>[31]</sup>, stating that incorporating silica in silicone elastomer results in an increase in equivalent elastic modulus but a net decrease in elongation at break. **Figure 11** illustrates the uniaxial tensile equivalent elasticity moduli of all batches, showing a clear distinction between unfilled and filled elastomers, with filled samples consistently displaying slightly higher moduli.

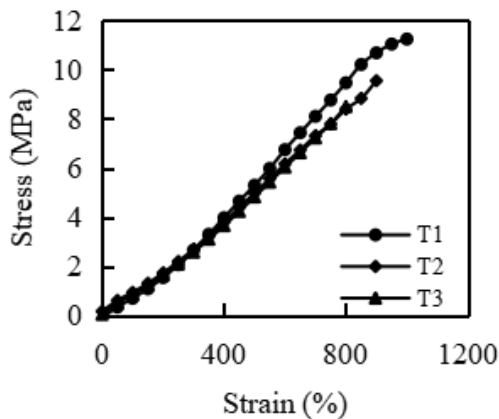


**Figure 10.** Uniaxial tensile test results.

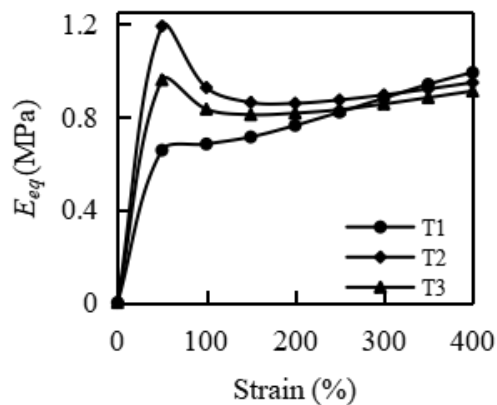


**Figure 11.** Uniaxial tensile elastic moduli.

Since the equivalent elastic modulus at 300% strain is considered a representative parameter for the tested elas-

tomers, reflecting the stiffness of the material under significant deformation, the values of the equivalent elastic moduli shown in **Figure 11** are summarized in **Table 3**.

**Table 3.** Uniaxial tensile moduli at 300% strain.

No.	Eq. Modulus (MPa)
T1	0.88
T2	0.90
T3	0.86

Hence, uniaxial tensile tests revealed a trade-off between stiffness and ductility, as indicated by the reduction in tensile strength and elongation at break. Although fumed silica filler enhanced hardness and equivalent elastic modulus, the reduction in elongation at break highlights the negative impact of increasing stiffness on ductility. The stronger chemical interactions between the crosslinked silicone polymer chains provided by the reinforcing filler ensure a higher deformation resistance. However, they restrict the stretching capacity of the chains, which leads to a restriction of movement in the polymer structure and a smaller deformation capacity of the elastomer. However, the stability of the equivalent elastic modulus up to 400% strain for all batches suggests that the material retains its integrity under comprehensive deformation, ensuring consistent performance under most loading conditions.

## 4.2. Lap Shear Tests

The tests were performed to measure the shear force and displacement behavior of the laminated samples. The results provide insights into the capacity of fumed silica reinforcement to improve the shear resistance of the tested silicone elastomeric laminations.

The double lap shear tests enabled observing the shear behavior of elastomers with varying filler proportions under simple shear loading conditions. The key results include the shear stress versus shear strain behavior, shear strength, and shear strain at break. **Figure 12** depicts the average shear stress-strain curves for the three lap shear test batches.

Although the shear coefficients of the batches increased slightly with increasing filler proportion, there was no drastic trend in their variation. The observed maximum shear strengths averaged 3.50 MPa, while the ultimate shear strains averaged 500%.

From the experiment data plotted in **Figure 12**, the

arithmetic means of the equivalent shear coefficients, key parameters for estimating the shear performances of the tested samples, which represent the capacity of the lamination to handle shear forces, were extracted and are summarized in **Figure 13**.

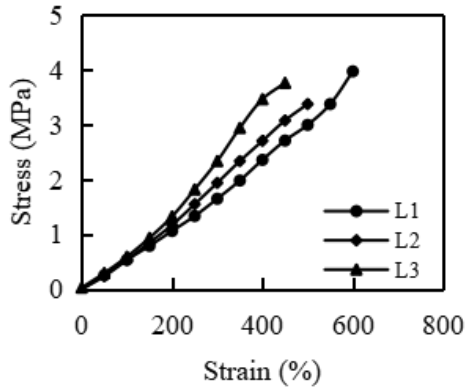


Figure 12. Lap shear test results.

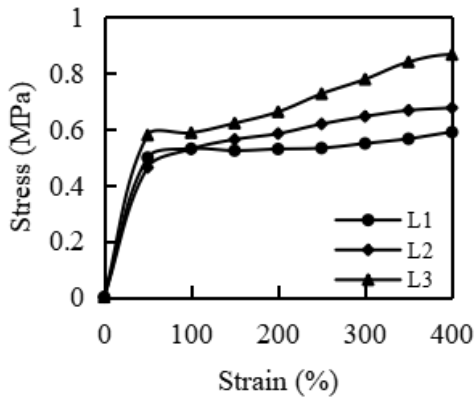


Figure 13. Lap shear moduli.

The arithmetic means of the equivalent shear moduli at 300% strain, representing the behavior of the tested samples under large shear deformations, are summarized in **Table 4**.

Table 4. Lap shear moduli at 300% strain.

No.	Eq. Shear Modulus (MPa)
L1	0.55
L2	0.65
L3	0.78

The lap shear tests showed no significant trend in either shear strength or shear strain at failure with varying filler proportions. This finding suggests that although fumed silica reinforcement improves the specific mechanical properties of the material, its effect on shear performance is less pronounced in laminated configurations. As a reference, the AASHTO M251<sup>[51]</sup> recommends elastomeric materials with shear coefficients between 0.55 MPa and 1.21 MPa for elastomeric bearings. The equivalent shear coefficients, which remained consistent across all samples, further reinforced this observation, indicating that the filler content did not substantially affect the shear capacity of the laminates.

### 4.3. Seismic Performance of Bearing Prototypes

The hysteresis loops obtained from the quasi-static test data, as displayed in **Figure 14**, exhibit the typical characteristics of elastomeric materials, with noticeable nonlinear behavior and energy dissipation.

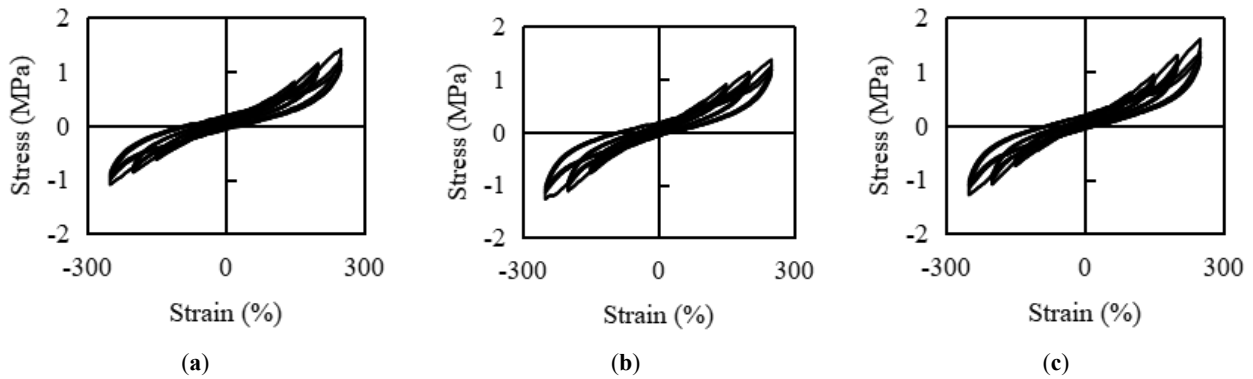
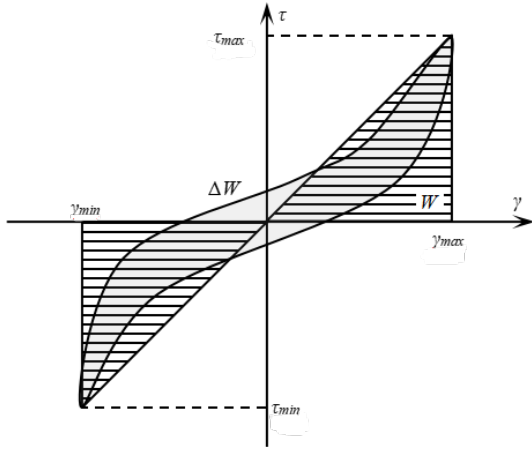


Figure 14. Bearing sample hysteretic curves: (a) P1, (b) P2, and (c) P3.

The equivalent shear coefficients and equivalent damping ratios of the prototypes were derived from the hysteresis data provided in **Figure 14**. Equation (3) was used to calculate equivalent shear coefficients, while Equation (4), based on the concept shown in **Figure 15**, was used to determine the damping ratios. The calculated values were then used to draw the curves shown in **Figure 16**, respectively.



**Figure 15.** Dissipated energy and hyperelastic potential energy of a hysteresis model.

$$\Delta W = \oint \tau d\gamma \quad (1)$$

$$W = \frac{1}{2} (\tau_{max}\gamma_{max} + \tau_{min}\gamma_{min}) \quad (2)$$

$$G_{eq} = \frac{\Delta\tau}{\Delta\gamma} \quad (3)$$

$$h_{eq} = \frac{1}{2\pi} \frac{\Delta W}{W} \quad (4)$$

Where,  $\Delta W$  represents the area delimited by the hysteresis curve,  $W$  is the elastic potential energy defined between the extreme stresses  $\tau_{min}$  and  $\tau_{max}$ , and the extreme strains  $\gamma_{min}$  and  $\gamma_{max}$ .

The equivalent shear coefficients ranged between 0.40 MPa and 0.60 MPa, whereas the damping ratios ranged from 4.50% to 7.00%. The variation of the filler proportion did not show a noticeable impact on both parameters, although a slight increase in the equivalent shear coefficient could be observed.

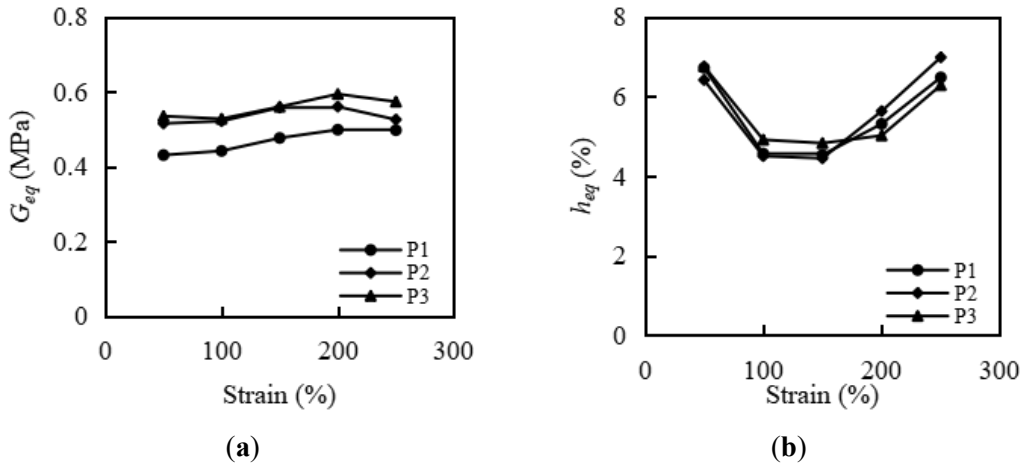


**Figure 16.** Equivalent elastic parameters: (a) equivalent shear coefficient and (b) equivalent damping ratio.

Quasi-static tests on the bearing prototypes demonstrated a typical nonlinear hysteresis behavior, with noticeable energy dissipation across all configurations. The equivalent shear coefficients and damping ratios derived from the hysteresis loops showed limited variation with filler proportions, indicating that while fumed silica reinforcement improves material stiffness, it does not significantly affect the damping or shear behavior at the bearing level. To illus-

trate the behavior of the tested bearing prototypes at large strains, **Table 5** reports the values of these key parameters at 250% strain. Based on the reported experimental results, a filler proportion of 1.25 phr was found to provide a balanced improvement in stiffness, tensile, and shear properties, making it an optimal composition for bearing applications. This specific formulation ensures enhanced mechanical performance while maintaining the workability and inherent

benefits of the silicone elastomers.

**Table 5.** Equivalent shear coefficient and damping ratio at 250% strain.

	Shear Coefficient (MPa)	Damping Ratio (%)
P1	0.50	6.49
P2	0.53	6.99
P3	0.57	6.29

The equivalent shear coefficients ranged between 0.50 MPa and 0.57 MPa, while the damping ratios ranged from 6.29% to 6.99% at 250% strain, as summarized in **Table 5**. These values are consistent with those observed from the lap shear tests, accounting for additional horizontal stresses induced by the constant vertical compression. For instance, Murota et al.<sup>[52]</sup> observed similar shear coefficients (0.392 MPa–0.62 MPa) in high damping rubber bearings at 100% strain. Similarly, Maghsoudi-Barmi, Khaloo and Ehteshami Moeini<sup>[14]</sup> reported damping ratios between 4.93% and 7.75% for steel-reinforced elastomeric bearings. However, unlike these studies, which primarily focused on conventional elastomers, the current research highlights the potential of fumed silica-reinforced silicone elastomers for seismic isolation applications.

The variation of the filler proportion did not show a drastic impact on either parameter, although a slight increase in the equivalent shear coefficient could be observed, rising from 0.50 MPa (P1) to 0.57 MPa (P3). This finding aligns with Abedi Koupai, Bakhshi and Valadoust Tabrizi<sup>[39]</sup>, who reported an increase in shear modulus with higher filler content in carbon black-reinforced elastomers for seismic isolator compounds. The relatively modest improvement in shear performance observed in this study may be attributed to the unique interaction between fumed silica and the silicone polymer matrix, which differs from the behavior of conventional fillers like carbon black on natural rubber.

Similarly, the damping ratios did not show pronounced variation across all filler proportions, ranging from 6.29% (P3) to 6.99% (P2), indicating that fumed silica reinforcement does not significantly alter the damping capacity of the material. This result is consistent with the findings of Abedi Koupai, Bakhshi and Valadoust Tabrizi<sup>[39]</sup>, who also observed that filler reinforcement only slightly improves the damping properties of elastomers.

## 5. Conclusions and Future Works

The results of this study provide insights into the impact of fumed silica as a reinforcing filler in silicone elastomeric bearings for seismic isolation applications, shedding light on several key aspects and implications for their design and application in seismic isolation systems.

The research question was successfully addressed by demonstrating that fumed silica reinforcement significantly enhances the stiffness and shear resistance of silicone elastomers while maintaining moderate damping properties. The findings confirm that fumed silica is an effective filler for improving the mechanical performance of silicone elastomers in seismic isolation applications.

The research objectives were accomplished by systematically evaluating the influence of varying fumed silica proportions (0, 1.25, and 2.50 phr) on the mechanical properties of silicone elastomers.

- (1) Fumed silica reinforcement significantly enhanced stiffness, as demonstrated by an increase in Shore A hardness from 21 (unfilled) to 49 (1.25 phr) and 56 (2.50 phr), representing a maximum improvement of 167%. This finding confirms the strong reinforcing effect of fumed silica on silicone elastomers.
- (2) A trade-off was observed in tensile behavior, with tensile strength decreasing from 11.25 MPa (unfilled) to 9.55 MPa (1.25 phr) and 8.50 MPa (2.50 phr), corresponding to reductions of 15% and 24%, respectively. Similarly, elongation at break declined, with maximum strains reducing from over 1,000% (unfilled) to 900% (1.25 phr) and 800% (2.50 phr), indicating losses of 10% and 20%, respectively. Despite this, the equivalent elastic modulus remained consistent up to 400% strain, suggesting that stiffness is preserved under most working conditions.
- (3) Lap shear tests revealed an improvement in shear resistance, with the equivalent shear modulus at 300% strain, increasing from 0.55 MPa (unfilled) to 0.65 MPa (1.25 phr) and 0.78 MPa (2.50 phr), representing relative increases of 18% and 42%, respectively. These findings indicate that fumed silica reinforcement enhances the ability of the elastomers to withstand shear forces, though the improvement is moderate.
- (4) Quasi-static tests on reduced scale bearing prototypes ex-

hibited inelastic behavior, with small increases in equivalent shear coefficients from 0.40 MPa (unfilled) to 0.45 MPa (1.25 phr) and 0.50 MPa (2.50 phr), representing improvements of 12.5% and 25%, respectively. Additionally, the damping ratio increased from 4.50% (unfilled) to 5.25% (1.25 phr) and 6.00% (2.50 phr), reflecting relative increases of 16.7% and 33.3%, respectively. These results suggest that while fumed silica reinforcement contributes to increased stiffness and shear resistance, its effect on damping capacity remains limited.

The experimental investigation validated all the hypotheses. (1) Increasing fumed silica content enhanced the stiffness of silicone elastomers, as evidenced by higher Shore A hardness values. (2) Incorporating fumed silica reduced tensile strength and elongation at break, indicating a trade-off between stiffness and ductility. (3) Fumed silica-reinforced silicone elastomers exhibited improved shear performance, with increased equivalent shear modulus and damping capacity under quasi-static loading conditions.

Thus, the research fills a gap in the existing literature by comprehensively evaluating the seismic isolation performance of fumed silica-reinforced silicone elastomers. While previous studies have focused on the general mechanical properties of fumed silica-reinforced elastomers, this study is among the first to investigate their behavior in laminated elastomeric bearings under seismic loading conditions. The findings contribute to understanding how filler reinforcement can be optimized for seismic isolation applications, particularly in harsh environmental conditions.

Moreover, the study has important theoretical and practical implications. From a theoretical perspective, it provides new insights into the role of fumed silica as a reinforcing filler in silicone elastomers, particularly in terms of its impact on stiffness, shear resistance, and damping properties. Practically, the findings offer a scientific basis for optimizing elastomer formulations for seismic isolation bearings, ensuring greater durability and resilience of structures in earthquake-prone regions. The results suggest that a filler proportion of 1.25 phr provides a balanced improvement in stiffness, tensile, and shear properties, making it an optimal composition for bearing applications.

Alongside the advancements demonstrated in silicone elastomer bearings, certain limitations persist in their design, fabrication, and application.

- (1) The experiments were conducted under controlled laboratory conditions, which may not fully replicate the complex and variable environments encountered during real-world seismic events. Future research should address these limitations by incorporating more realistic testing conditions that simulate the complex and variable nature of seismic events.
- (2) While the mechanical properties of the samples were evaluated and measured, their dynamic behavior in realistic conditions was not examined in this study. Investigating the dynamic behavior of the samples will yield a more comprehensive understanding of their suitability for seismic isolation purposes.
- (3) The long-term durability of fumed silica-reinforced silicone elastomers requires further investigation. Moisture uptake may affect the mechanical performance, adhesion, and aging behavior of these materials, potentially influencing their long-term efficiency in seismic isolation systems. Future studies will include liquid absorption tests to assess the resistance of the elastomers to moisture and other environmental factors. Traditional liquid absorption methods are often labor-intensive and time-consuming; therefore, novel techniques, such as automated weight measurement<sup>[53]</sup> and computer vision-based analysis<sup>[54]</sup>, will be explored to improve the accuracy and efficiency of liquid absorption characterization.

## Author Contributions

A.R.: literature review, experimental investigation, data processing, and first draft; J.D.: conceptualization, design of experiments, editing, and proofreading.

## Funding

This study received no external funding.

## Institutional Review Board Statement

Not applicable.

## Informed Consent Statement

Not applicable.

## Data Availability Statement

The data used to support the findings of this study are included within the article.

## Conflict of Interest

This research does not have any conflict of interest.

## References

- [1] Altalabani, D., Hejazi, F., 2023. Development of rectangular vibration isolators with double core systems for structures. *International Journal of Civil Engineering*. 21, 763–787. DOI: <https://doi.org/10.1007/s40999-022-00801-5>
- [2] Salvatori, A., Bongiovanni, G., Clemente, P., et al., 2022. Observed seismic behavior of a HDRB and SD isolation system under far fault earthquakes. *Infrastructures*. 7(2), 13. DOI: <https://doi.org/10.3390/infrastructures7020013>
- [3] Peng, T., Dong, Y., 2023. Seismic responses of aqueducts using a new type of self-centering seismic isolation bearing. *Sustainability*. 15(3), 2402. DOI: <https://doi.org/10.3390/su15032402>
- [4] Yin, Z., Sun, H., Jing, L., et al., 2022. Geotechnical seismic isolation system based on rubber-sand mixtures for rural residence buildings: Shaking table test. *Materials*. 15(21), 7724. DOI: <https://doi.org/10.3390/ma15217724>
- [5] Pan, P., Shen, S., Shen, Z., et al., 2018. Experimental investigation on the effectiveness of laminated rubber bearings to isolate metro generated vibration. *Measurement (Lond)*. 122, 554–562. DOI: <https://doi.org/10.1016/j.measurement.2017.07.019>
- [6] Chen, B., Dai, J., Song, T., Guan, Q., 2022. Research and development of high-performance high-damping rubber materials for high-damping rubber isolation bearings: A review. *Polymers*. 14(12), 2427. DOI: <https://doi.org/10.3390/POLYM14122427>
- [7] Zhang, R.-j., Li, A.-q., 2020. Experimental study on temperature dependence of mechanical properties of scaled high-performance rubber bearings. *Composites Part B: Engineering*. 190, 107932. DOI: <https://doi.org/10.1016/j.compositesb.2020.107932>
- [8] Itoh, Y., Gu, H.S., 2009. Prediction of aging characteristics in natural rubber bearings used in bridges. *Journal of Bridge Engineering*. 14(2), 122–128. DOI: [https://doi.org/10.1061/\(ASCE\)1084-0702\(2009\)14:2\(122\)](https://doi.org/10.1061/(ASCE)1084-0702(2009)14:2(122))
- [9] Li, Y., Ma, Y., Zhao, G., et al., 2023. Study on the basic performance deterioration law and the application of lead rubber bearings under the alternation of aging and seawater erosion. *Buildings*. 13(2), 360. DOI: <https://doi.org/10.3390/buildings13020360>
- [10] Nishi, T., Murota, N., 2013. Elastomeric seismic-protection isolators for buildings and bridges. *Chinese Journal of Polymer Science (English Edition)*. 31, 50–57. DOI: <https://doi.org/10.1007/s10118-013-1217-8>
- [11] Zhang, Z.J., Zhang, Z.Q., Yue, S., et al., 2023. Performance characteristics of silicone rubber for use in acidic environments. *Polymers (Basel)*. 15(17), 3598. DOI: <https://doi.org/10.3390/polym15173598>
- [12] Han, R., Li, Y., Zhu, Q., et al., 2022. Research on the preparation and thermal stability of silicone rubber composites: A review. *Composites Part C: Open Access*. 8, 100249. DOI: <https://doi.org/10.1016/j.jcomc.2022.100249>
- [13] Shit, S.C., Shah, P., 2013. A review on silicone rubber. *National Academy Science Letters*. 36, 355–365. DOI: <https://doi.org/10.1007/s40009-013-0150-2>
- [14] Maghsoudi-Barmi, A., Khaloo, A., Ehteshami Moeini, M., 2021. Experimental investigation of unbonded ordinary steel reinforced elastomeric bearings as an isolation system in bridges. *Structures*. 32, 604–616. DOI: <https://doi.org/10.1016/j.istruc.2021.02.055>
- [15] Wang, Z., Lin, Y., Li, Z., et al., 2023. Effect of fluorosilicone rubber on mechanical properties, dielectric breakdown strength and hydrophobicity of methyl vinyl silicone rubber. *Polymers (Basel)*. 15(16), 3448. DOI: <https://doi.org/10.3390/polym15163448>
- [16] Clet, J.A.G., Liou, N.S., Weng, C.H., et al., 2022. A parametric study for tensile properties of silicone rubber specimen using the bowden-type silicone printer. *Materials*. 15(5), 1729. DOI: <https://doi.org/10.3390/ma15051729>
- [17] Wei, C., Hao, X., Mao, C., et al., 2023. The mechanical properties of silicone rubber composites with shear thickening fluid microcapsules. *Polymers (Basel)*. 15(12), 2704. DOI: <https://doi.org/10.3390/polym15122704>
- [18] Yelemessov, K., Sabirova, L.B., Martyushev, N.V., et al., 2023. Modeling and model verification of the stress-strain state of reinforced polymer concrete. *Materials*. 16(9), 3494. DOI: <https://doi.org/10.3390/ma16093494>
- [19] Zhang, Y., Liu, W., Zhou, Q., et al., 2023. Effects of vinyl functionalized silica particles on thermal and mechanical properties of liquid silicone rubber nanocomposites. *Polymers (Basel)*. 15(5), 1224. DOI: <https://doi.org/10.3390/polym15051224>
- [20] Wang, J., Jia, H., 2022. The Effects of Carbon–silica dual-phase filler on the crosslink structure of natural rubber. *Polymers (Basel)*. 14(18), 3897. DOI: <https://doi.org/10.3390/polym14183897>
- [21] Jung, J.K., Lee, C.H., Son, M.S., et al., 2022. Filler effects on H<sub>2</sub> diffusion behavior in nitrile butadiene rubber blended with carbon black and silica fillers of

- different concentrations. *Polymers (Basel)*. 14(4), 700. DOI: <https://doi.org/10.3390/polym14040700>
- [22] Gupta, S., Esmaeeli, H.S., Moini, R., 2024. Tough and ductile architected nacre-like cementitious composites. *Advanced Functional Materials*. 34(39), 2313516. DOI: <https://doi.org/10.1002/adfm.202313516>
- [23] K. C. N., Abraham, J., Thomas, M.G., et al., 2024. Carbon nanotube filled rubber nanocomposites. *Frontiers in Carbon*. 3, 1339418. DOI: <https://doi.org/10.3389/frcarb.2024.1339418>
- [24] Zhao, R.P., Yin, Z.G., Zou, W., et al., 2023. Preparation of high-strength and excellent compatibility fluorine/silicone rubber composites under the synergistic effect of fillers. *ACS Omega*. 8(4), 3905–3916. DOI: <https://doi.org/10.1021/ACSOMEGA.2C06489>
- [25] Barrera, C.S., Cornish, K., 2017. Processing and mechanical properties of natural rubber/waste-derived nano filler composites compared to macro and micro filler composites. *Ind Crops Prod*. 107, 217–231. DOI: <https://doi.org/10.1016/J.INDCROP.2017.05.045>
- [26] Dasaesamoh, A., Khotmungkhun, K., Subannajui, K., 2023. Natural rigid and hard plastic fabricated from elastomeric degradation of natural rubber composite with ultra-high magnesium carbonate content. *Polymers (Basel)*. 15(14), 3078. DOI: <https://doi.org/10.3390/polym15143078>
- [27] Bukit, N., Ginting, E.M., Sidebang, E., et al., 2020. Mechanical properties of natural rubber compounds with oil palm boiler ash and carbon black as a filler. *Journal of Physics: Conference Series*. 1428, 012020.
- [28] Wang, X., Qin, Y., Zhao, C., 2022. High-temperature behavior of silicone rubber composite with boron oxide/calcium silicate. *E-Polymers*. 22, 595–606. DOI: <https://doi.org/10.1515/epoly-2022-0051>
- [29] Feng, L., Zhou, L., Feng, S., 2016. Preparation and characterization of silicone rubber cured via catalyst-free aza-Michael reaction. *RSC Advances*. 6, 111648–111656. DOI: <https://doi.org/10.1039/C6RA23016D>
- [30] Dall'Asta, A., Ragni, L., 2006. Experimental tests and analytical model of high damping rubber dissipating devices. *Engineering Structures*. 28, 1874–1884. DOI: <https://doi.org/10.1016/j.engstruct.2006.03.025>
- [31] Jiang, S., Yong, Z., 2024. Modulation of mechanical properties of silica-filled silicone rubber by cross-linked network structure. *Polymers*. 16, 2304. DOI: <https://doi.org/10.3390/POLYM16162304>
- [32] Dorigato, A., D'Amato, M., Pegoretti, A., 2012. Thermo-mechanical properties of high density polyethylene - Fumed silica nanocomposites: Effect of filler surface area and treatment. *Journal of Polymer Research*. 19, 1–11. DOI: <https://doi.org/10.1007/S10965-012-9889-2>
- [33] Rao, V.V., Dixit, P., Krishna, R.H., Murthy, K.R., 2023. Performance evaluation of nano MgO filled polymer material for high voltage insulation. *Journal of Surface Investigation*. 17, 94–103. DOI: <https://doi.org/10.1134/S1027451023010263>
- [34] Donnet, J.-B., Bansal, R.C., Wang, M.-J., 1993. Carbon black : Science and technology, 2nd ed. Routledge: New York, NY, USA. pp. 289–356.
- [35] Liang, T., Yan, C., Zhou, S., et al., 2017. Carbon black reinforced polymethyl methacrylate (PMMA)-based composite particles: Preparation, characterization, and application. *Journal of Geophysics and Engineering*. 14, 1225–1232. DOI: <https://doi.org/10.1088/1742-2140/aa6e7e>
- [36] Irez, A.B., Bayraktar, E., Miskioglu, I., 2020. Fracture toughness analysis of epoxy-recycled rubber-based composite reinforced with graphene nanoplatelets for structural applications in automotive and aeronautics. *Polymers (Basel)*. 12(2), 448. DOI: <https://doi.org/10.3390/polym12020448>
- [37] Sun, X., Guo, R.F., Shaga, A., et al., 2020. Preparation and characterization of high damage-tolerance nacre-inspired magnesium alloy matrix composites with high carbon nanotube contents. *Carbon*. 162, 382–391. DOI: <https://doi.org/10.1016/j.carbon.2020.02.072>
- [38] Norouznezhad, M., Janani, H., 2024. Cross-linking network topology and durability in silicone rubber sealants for PEMFCs: The impact of curing systems and nanosilica interactions. *Journal of Polymer Research*. 31, 1–17. DOI: <https://doi.org/10.1007/S10965-024-03898-5>
- [39] Abedi Koupai, S., Bakhshi, A., Valadoust Tabrizi, V., 2017. Experimental investigation on effects of elastomer components on dynamic and mechanical properties in seismic isolator compounds. *Constr Build Mater*. 135, 267–278. DOI: <https://doi.org/10.1016/j.conbuildmat.2016.12.184>
- [40] Pöschl, M., Vašina, M., Zádrapa, P., et al., 2020. Study of carbon black types in SBR rubber: Mechanical and vibration damping properties. *Materials*. 13(10), 2394. DOI: <https://doi.org/10.3390/ma13102394>
- [41] Rutherford, K.J., Akutagawa, K., Ramier, J.L., et al., 2023. The Influence of Carbon Black Colloidal Properties on the Parameters of the Kraus Model. *Polymers (Basel)*. 15(7), 1675. DOI: <https://doi.org/10.3390/polym15071675>
- [42] Ariati, R., Sales, F., Souza, A., et al., 2021. Polydimethylsiloxane composites characterization and its applications: A review. *Polymers (Basel)*. 13(23), 4258.
- [43] Rubio-Mateos, A., Rivero, A., Ukar, E., et al., 2020. Influence of elastomer layers in the quality of aluminum parts on finishing operations. *Metals (Basel)*. 10(2), 289. DOI: <https://doi.org/10.3390/met10020289>
- [44] Vacalebri, M., Frison, R., Corsaro, C., et al., 2023. Current state of the art and next generation of materials for a customized intraocular lens according to a patient-specific eye power. *Polymers*. 15(6), 1590.
- [45] Boldridge, D., 2010. Morphological characterization

- of fumed silica aggregates. *Aerosol Science and Technology*. 44(3), 182–186. DOI: <https://doi.org/10.1080/02786820903499462>
- [46] Jin, Y., Zheng, X., Wang, L., et al., 2020. Improved mechanical properties of natural rubber composites reinforced by novel SiO<sub>2</sub>@HCNFs nanofillers at a low filler loading. *Journal of Applied Polymer Science*. 137(40), 49225. DOI: <https://doi.org/10.1002/ap.49225>
- [47] Haddad, Y.M., Feng, J., 2003. On the trade-off between damping and stiffness in the design of discontinuous fibre-reinforced composites. *Composites Part B: Engineering*. 34, 11–20. DOI: [https://doi.org/10.1016/S1359-8368\(02\)00076-8](https://doi.org/10.1016/S1359-8368(02)00076-8)
- [48] ASTM, 2015. ASTM D2240-15. Standard Test Method for Rubber Property-Durometer Hardness. ASTM: West Conshohocken, PA, USA. DOI: <https://doi.org/10.1520/D2240-15>
- [49] ASTM, 2006. ASTM D412-06. Standard Test Methods for Vulcanized Rubber and Thermoplastic Elastomers - Tension. ASTM: West Conshohocken, PA, USA.
- [50] JIS, 2010. JIS K 6251. Test Method for Vulcanized Rubber - Tensile Test. JIS: Tokyo, Japan.
- [51] AASHTO, 2016. AASHTO M251 06. Standard Specification for Plain and Laminated Elastomeric Bridge Bearings. AASHTO: Washington, DC, USA.
- [52] Murota, N., Suzuki, S., Mori, T., et al., 2021. Performance of high-damping rubber bearings for seismic isolation of residential buildings in Turkey. *Soil Dynamics and Earthquake Engineering*. 143, 106620. DOI: <https://doi.org/10.1016/j.soildyn.2021.106620>
- [53] Sabir, B.B., Wild, S., O'farrell, M., 1998. A water sorptivity test for mortar and concrete. 31, 568–574. DOI: <https://doi.org/10.1007/BF02481540>
- [54] Kabir, H., Wu, J., Dahal, S., et al., 2024. Automated estimation of cementitious sorptivity via computer vision. *Nature Communications*. 15, 9935. DOI: <https://doi.org/10.1038/s41467-024-53993-w>